ARTICLE

Transferrable Superhydrophobic Surface Constructed by a Hexagonal CuI Powder without Modification by Low-Free-Energy Materials

Shuyan Gao,*,† Zhengdao Li,† Shuxia Yang,† Kai Jiang,† Yue Li,*,‡ Haibo Zeng,‡ Liang Li,‡ and Hongqiang Wang‡

College of Chemistry and Environmental Science, Henan Normal University, 46 Jianshe Street, Xinxiang, 453007 Henan, People's Republic of China, and Key Lab of Materials Physics, Anhui Key Laboratory of Nanomaterials and Nanotechnology, Institute of Solid State Physics, Chinese Academy of Sciences, Hefei, 230031 Anhui, People's Republic of China

ABSTRACT A new route combining a facile wet-chemical process and spin coating was developed to fabricate a CuI film assembled by hexagonal crystals. Remarkably, such a CuI film displays excellent superhydrophobicity without further modification by low-free-energy materials (thiol or fluoroalkylsilane). The special wettability is attributed to a hierarchical morphology of CuI crystals with two length-scale roughnesses and the nature of the material itself. Importantly, this superhydrophobicity is quite stable and the water contact angle of the as-prepared sample only decreases slightly, even when it is kept in air for about half a year. The superhydrophobicity of the as-prepared CuI powder is a bulk property of the material and not just of its surface, so such a powder coating could then prove useful in conferring superhydrophobicity to other surfaces to which it is applied. These facts might improve its practical application with environmental friendship in superhydrophobic coatings.

KEYWORDS: transferrable superhydrophobic surface • hexagonal CuI powder • modification • low-free-energy materials

1. INTRODUCTION

Superhydrophobic surfaces whose water contact angle (CA) is larger than 150° have recently aroused great interest in numerous industrial and scientific fields because of their unique water repellence with self-cleaning properties and their potential for practical applications in multiple fields, including self-cleaning windshields for automobiles, impermeable textiles, antisticking coatings for antennas and windows against snow, microfluidics in biotechnology, antibiofouling paints, and the biomedical area (1−21). Nature accomplishes such fascinating superhydrophobic effects by combining the use of low-surface-energy materials with surfaces that demonstrate peculiar features, such as micro- and nanosized hierarchical roughness (22−25). Well-known examples include self-cleaning lotus leaves and water striders that are able to walk on the water surface. Inspired by Nature, considerable efforts concerning the study of such surfaces have been made and a number of approaches to artificial superhydrophobic surfaces have been developed (26−42). Generally, a superhydrophobic surface can be effectively fabricated by combining the appropriate surface roughness with materials of low surface energy, and the modification of compounds that contain fluorine or thiol is often necessary (43−45). However, there are several issues originating from the modification of fluorine- or thiol-containing compounds, i.e., multistep procedures, harsh modification conditions, an environmentally unfriendly fluorine- or thiol-containing compound and its contamination, and, most importantly, the instability of the superhydrophobic effect. As a result, practical applications of such functional materials have not been fully realized, and there is a clear need for an applicable approach toward superhydrophobic surfaces without modification by low-free-energy materials. The preparation of superhydrophobic surfaces without further modification with low-free-energy materials is a formidable challenge, and the development of such a surface has rarely been reported.

Recently, cuprous iodide (CuI) has attracted much attention because of its unusual features (46−51), such as a large direct band gap (3.1 eV below 350 °C), a negative spin−orbit splitting, anomalous diamagnetism behavior, a large ionicity, a new high-pressure phase, and potential applications in a superionic conductor, solid-state solar cells, catalysis for the synthesis of organic compounds, etc. Consequently, great efforts have been made to establish different techniques to prepare CuI nano/microparticles (52−59), such as electrodeposition, a pulse laser deposition technique, vacuum evaporation, a hydro-/solvothermal method, and an in situ etching process. Except for all of these investigations, the fabrication and use of CuI with special structures in the

* E-mail: shuyangao@henannu.edu.cn (S.G.), yueli@issp.ac.cn (Y.L.).
Received for review July 12, 2009 and accepted August 31, 2009
† Henan Normal University.
‡ Chinese Academy of Sciences.
DOI: 10.1021/am900466f

Published on Web 09/15/2009

wettability field have never been studied despite its outstanding advantages, such as high safety, environmental benignity, low cost, etc. (60−62). In this work, we develop a new route to fabricate a CuI film consisting of hexagonal-shaped CuI crystals by a facile wet-chemical process. Interestingly, such a CuI film demonstrates excellent superhydrophobicity with a water CA of 157.3° without further modification by low-free-energy materials. More importantly, this superhydrophobicity was so stable that the water CA of the as-prepared sample only decreased slightly, even when it was kept in air for about half a year. Additionally, the superhydrophobicity of the as-prepared CuI powder is not just of its surface but a bulk property of the material, which makes it useful in conferring superhydrophobicity to other applied surfaces. These facts might lead to its good practical application with environmental friendship in superhydrophobic coatings.

2. EXPERIMENTAL SECTION

All chemical reagents of analytical grade were supplied by Beijing Chemicals Co. Ltd. and used as received. All water used in this investigation was deionized by a Nanopure filtration system to a resistivity of 18 MΩ·cm. The preparation of a hexagonal CuI powder is quite straightforward. A total of 5 mL of a 0.15 M cupric sulfate aqueous solution, 6 mL of 5 mM aniline, and 5 mL of a 0.15 M potassium iodide aqueous solution were added under constant stirring, respectively, to 14 mL of ultrapure water. The mixture was stirred for 10 min in a 50 mL round-bottomed flask at room temperature. Then a large quantity of dark-yellow precipitate and a colorless supernatant were obtained. The resulting precipitate was filtered, washed with distilled water, and redispersed in distilled water for further characterization with field-emission scanning electron microscopy (FESEM), transmission electron microscopy (TEM), high-resolution TEM (HRTEM), X-ray diffraction (XRD), and X-ray photoelectron spectroscopy (XPS) techniques to obtain detailed information on the morphology, components, and crystalline structure. The FESEM images were obtained on an XL30 ESEM FEG scanning electron microscope operating at 20 kV. TEM and HRTEM were taken with a JEOL JEM-2010 transmission electron microscope. The XRD pattern was recorded on a Ragaku-D/Max 2500 V/PC X-ray diffractometer using Cu $K\alpha_1$ radiation (λ = 1.540 56 Å) at 40 kV and 200 mA. XPS was collected on an ESCALab MKII X-ray photoelectron spectrometer, using non-monochromatized Mg Kα X-ray as the excitation source.

A droplet of the CuI particle suspension in ethanol was placed on a cleaned substrate fixed on a spin coater at a rotating speed of 800 rpm for 5 min, and a CuI crystal film would be formed after drying. The wettability of the as-prepared film was characterized by measuring the water CA with a contact angle meter. A 2 μL water droplet was placed on this hierarchical particle array film for water CA measurement. CA values were obtained by averaging five measurements on different areas of the sample surface.

3. RESULTS AND DISCUSSION

3.1. Structural Characterization. The phase purity of the as-prepared product was determined by XRD, as shown in Figure 1. All of the diffraction peaks can be readily indexed to cubic CuI (space group $F\bar{4}3m$, $a = b = c = 6.0510$ Å, $\alpha = \beta = \gamma = 90°$, and JCPDS file no. 06-0246). Parts a and b of Figure 2 show XPS spectra of Cu $2p_{1/2}$ and $2p_{3/2}$ and the I $^3d_5$ core level acquired from an as-prepared sample.

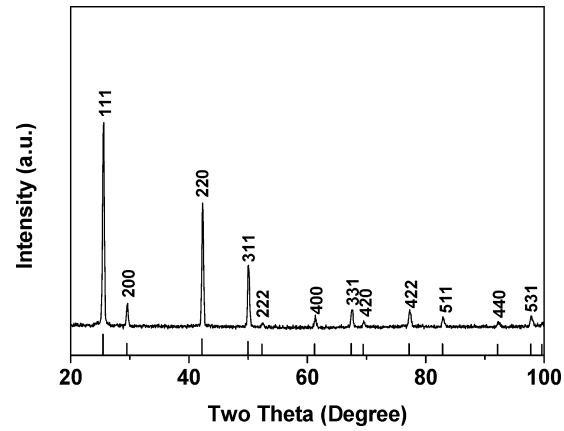

FIGURE 1. XRD patterns of the as-prepared sample. The vertical lines represent the data of JCPDS card no. 06-0246.

The positions of the peaks of Cu $2p_{1/2}$ and $2p_{3/2}$ of the sample are 952.2 and 932.2 eV, respectively, without the shake-up, which implies a feature of Cu^+ (63). The peak positions of I $^3d_5$, 619.5 and 631.0 eV, are well consistent with the ones in the database. What is worth noting is that the N 1s peak originating from the raw material, aniline, was also observed (Figure 2c), which is a firm proof that aniline participated in the formation of the product.

Low-magnification FESEM observations show that the panoramic morphology of the as-obtained CuI product is mainly a hexagonal sheet with side lengths from 0.4 to 1 μm (Figure 3A). Closer observation (Figure 3B) shows that each hexagonal sheet is built from six orthotrigonal sheets with discernible connection marks, which typically indicates that the connection mechanism functions here and will be discussed in the following section. A much closer examination (Figure 3C) vividly reveals that the structure of the architecture is assembled from a single layer of oriented nanorods with an average diameter of ca. 20 nm and a length of 300 nm, which results in a rough surface protruding to the outside. This observation shows that the surface possesses a hierarchical morphology with two length-scale roughnesses, which may endow it with improved wettability. The microstructure of the as-grown samples is further analyzed using TEM and HRTEM. The TEM image of a single nanocrystal (Figure 4A) reveals clearly a hexagonal morphology consisting of six trigonal sheets. The length of the side is around 0.45 μm. The HRTEM image in Figure 4B can give further insight into the details of the structure. The lattice fringes with d spacings of 3.41 and 2.27 Å corresponding to the {111} and {220} planes can be clearly distinguished, which indicates its single-crystalline nature. This result is well consistent with the XRD pattern.

3.2. Formation Mechanism. From FESEM observation, it can be clearly seen that each hexagonal CuI is built from six trigonal sheets, most of which are orthotrigonal. To the best of our knowledge, there are few reports on such a hexagonal morphology built from trigonal sheets. Let us tentatively discuss the formation mechanism. In this wet chemical process, aniline serves as the reducing agent for the reaction and Cu^{2+} ions are reduced and complex with I^- simultaneously to form CuI monomers. When the con-

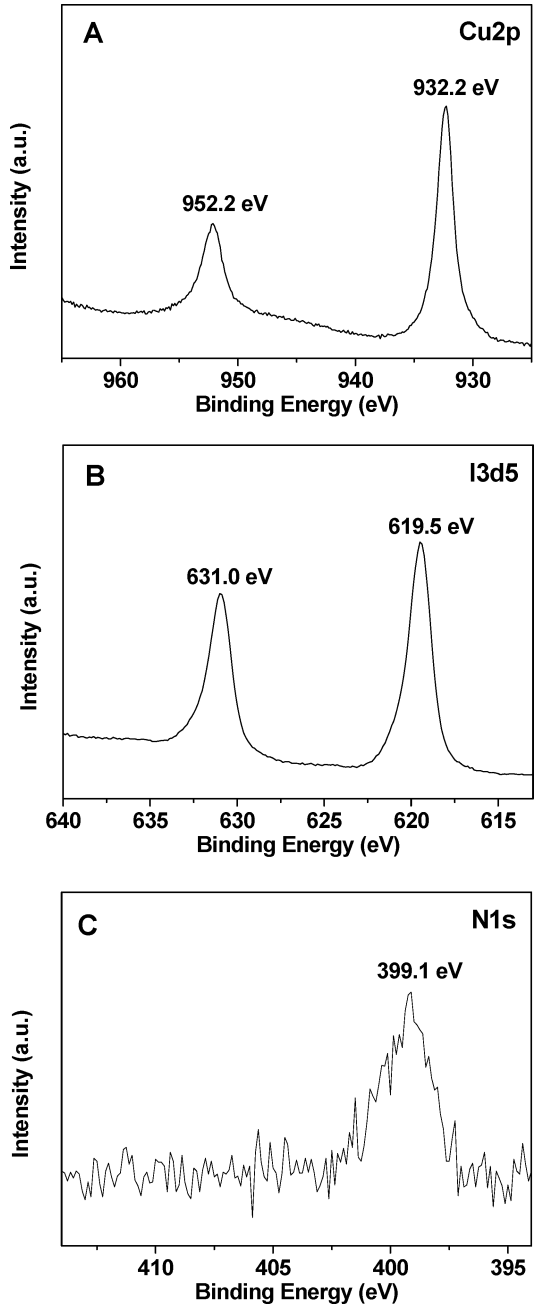

FIGURE 2. XPS spectra of the sample. Parts A–C are spectra from the Cu 2p, I $^3d_5$, and N 1s core levels, respectively.

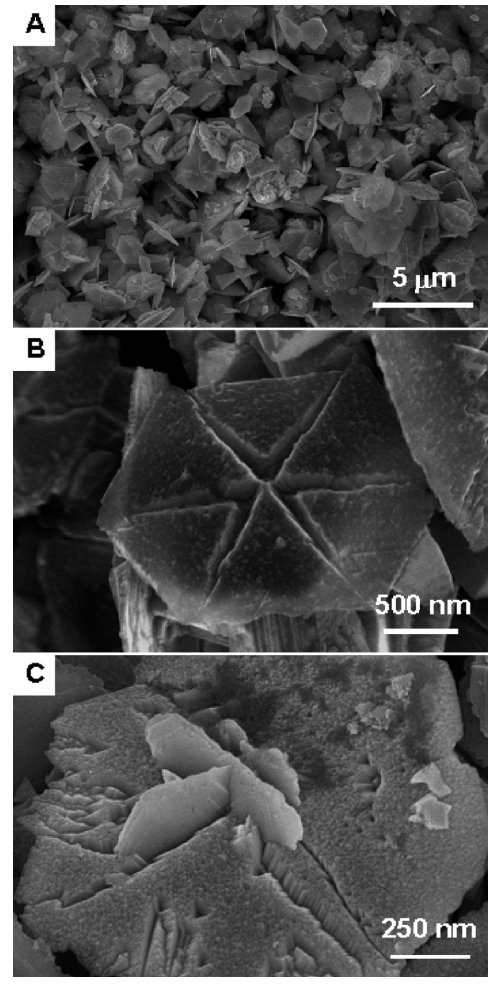

FIGURE 3. FESEM images of the as-prepared CuI: (A) low-magnification image; (B) a single hexagonal nanosheet; (C) high-magnification observation.

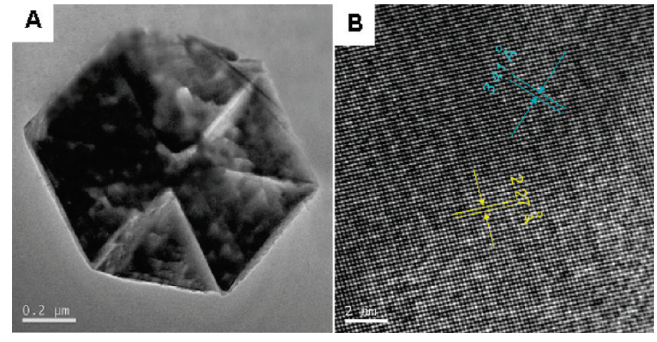

FIGURE 4. TEM (A) and HRTEM (B) images of the as-prepared CuI.

centration of CuI monomers has reached supersaturation, they start to nucleate and grow into particles, sheets, or wires. Here we suggest that, although the exact role of aniline is still not clear, aniline can be bonded to the CuI nucleation surface through the $-NH_2$ functional group, affecting the surface energy. Aniline molecules and/or some molecules induced by reaction adsorb preferentially onto the sites of the {111} planes of CuI nuclei, which greatly decreases the surface energy of the {111} planes and leads to preferential growth along the ⟨110⟩ directions. As a consequence, a rodlike intermediate formed. This, in turn, favors the formation of triangular or hexagonal CuI nanosheets. The participation of aniline in the formation of the hexagonal CuI sheet has been verified by XPS (Figure 2C). The failure to produce hexagonal CuI upon substitution of ascorbic acid and tryptophan for aniline further confirms the special role of aniline in the formation of such a unique hexagonal CuI (Figure 5).

On the basis of the above analysis, we believe that there are two main mechanisms for the formation of the large CuI nanosheets after the formation of a large number of small nanosheets under the proper conditions: (i) some of the small nanosheets will continue to grow mainly along the {110} direction, within the {111} planes, by CuI monomer attachment, forming larger nanosheets; (ii) most small nanosheets will be connected together along the {110}

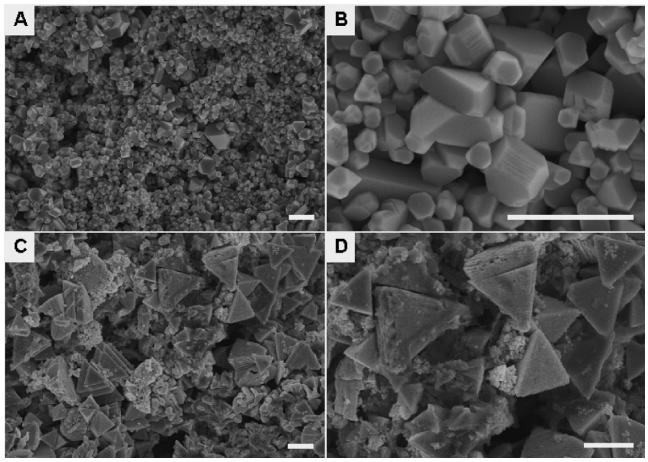

FIGURE 5. FESEM images of the products by substitution of ascorbic acid and tryptophan for aniline.

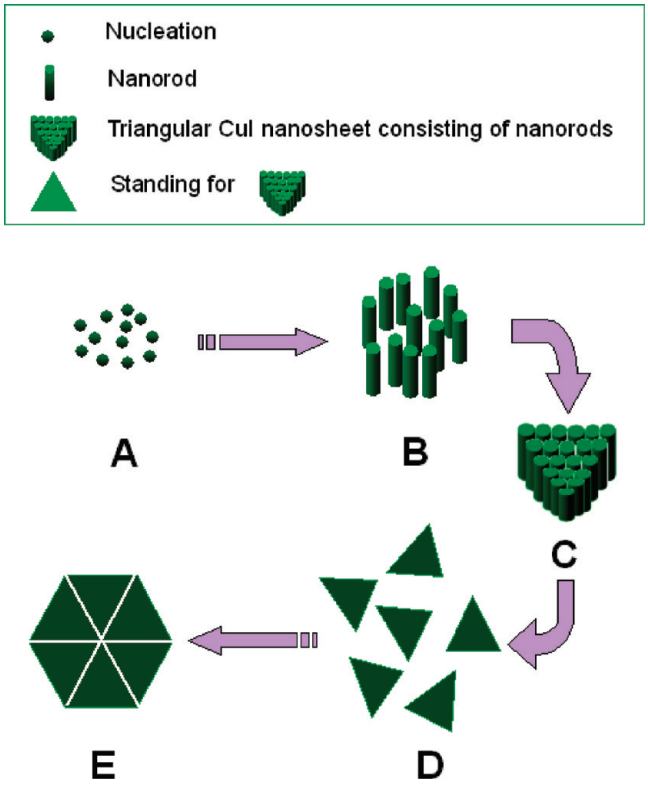

FIGURE 6. Schematic illustration for the formation of hexagonal nanosheets by the connection mechanism: (A) formation of CuI crystal seeds; (B) formation of nanorods; (C) self-assembly of nanorods into triangular nanosheets; (D and E) formation of hexagonal nanosheets by the connection mechanism from the formed triangular nanosheets.

lateral planes, which are of relatively high surface energy, leading to the formation of very large hexagonal nanosheets, as schematically illustrated in Figure 6. Obviously, such a connection should be thermodynamically more stable and hence will occur in solution during the reaction. In addition, such a growth mechanism had also been illustrated by Jin et al. (64) and Li et al. (65).

The connection mechanism was further examined by morphology investigation, as demonstrated in Figure 7. Both the incomplete and complete hexagonal nanosheets have discernible connection marks, which typically indicate the

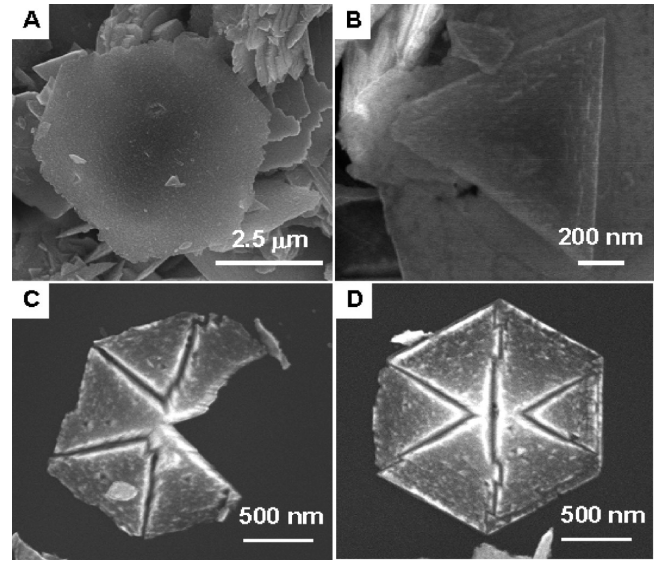

FIGURE 7. Some typical FESEM images of crystal growth by (A and B) atomic attachment and (C and D) by the connection among six triangular sheets. (A and B) Results of atomic attachment to the edge sides of a hexagonal sheet and a triangular sheet, respectively. (C and D) Incomplete and complete connections among hexagonal sheets, respectively.

connection among triangular sheets (see parts C and D of Figure 7, respectively). Also, we can see evidence of the growth mechanism known as "atomic attachment" in parts A and B of Figure 7, in which the structures display rough profiles, indicating that atoms attach to the edges during the reaction.

3.3. Superhydrophobic Surface without Modification by Low-Free-Energy Materials. Figure 8A shows an image of the water droplet on the CuI film by spin coating. One can see that the water drop almost displays a spherical shape. The water CA in this image is 157.3°. A sequence of photographs of a droplet lowered onto the surface was recorded to probe the CA hysteresis of the CuI film (Figure 8B–F). In this sequence, a clear comparison of the droplet shape is displayed for the initial state due to gravity, the exact contacting state, the tight and severe contacting states under pressure, and the state when removed from the substrate. When the droplet just touched the surface, it did not change from its initial shape.

Superhydrophobicity is usually explained by the Cassie–Baxter model (8) according to the fact that a rough hydrophobic surface can be considered as a kind of porous or hierarchical medium at which the penetration of the liquid is not favorable. Thus, air pockets remain trapped below the liquid, which sits above a patchwork of solid and air. As can be seen from the special hierarchical structure of the as-prepared sample shown in Figure 3, this kind of highly rough surface is mainly composed of air. It was then concluded that such a strong superhydrophobicity is due to the higher surface roughness caused by the unique hierarchical structures without surface treatment and is in agreement with previously reported results on a real superhydrophobicity with hierarchical micro/nanostructured surfaces (66–68). The relatively small water CAs (Figure 9) for other CuI films with morphologies such as those shown in Figure 5, 102.2°

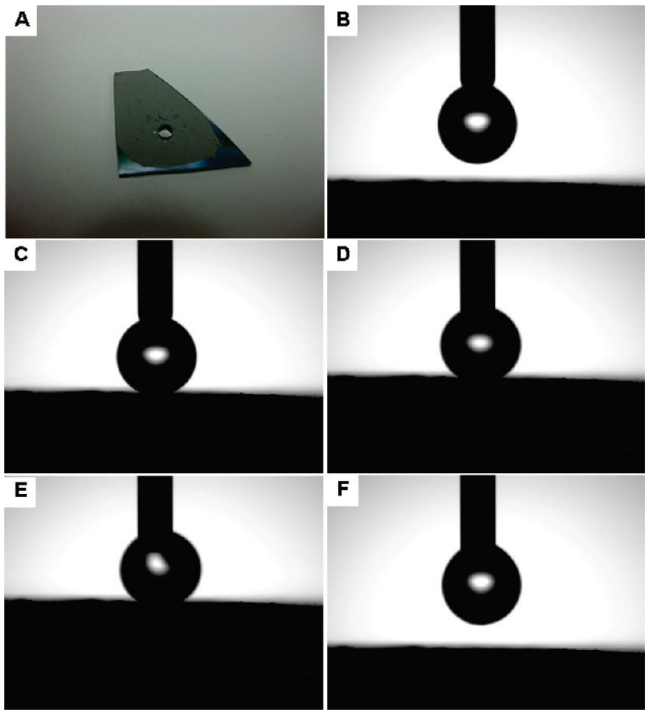

FIGURE 8. (A) Image of water on the CuI-coated silicon wafer. (B–D) Sequential photographs of the droplet recorded before and after the water droplet made contact with the CuI-coated silicon wafer: (B) initial state; (C) exact contact; (D) tight contact; (E) severe contact; (F) final state.

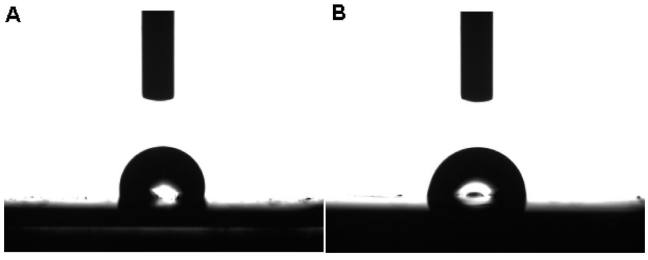

FIGURE 9. Water CAs on the products by substitution of ascorbic acid and tryptophan for aniline, as shown in Figure 5.

and 104.8°, respectively, give a firm proof that the excellent superhydrophobicity is ascribed to the unique hierarchical micro/nanostructures associated with the hexagonal CuI.

The long-term preservation of superhydrophobicity is an important criterion for real applications of superhydrophobic materials. In order to examine this parameter, a silicon wafer coated with the superhydrophobic layer of a CuI powder was kept in air for half a year. Figure 10 presents the water CA change with time when it was kept in air. The water CA decreased just slightly but still retained its superhydrophobicity, even after 6 months, which substantiates that the as-prepared sample possesses a very stable superhydrophobicity.

Because the superhydrophobicity of the as-prepared CuI powder is a bulk property of the material and not just of its surface, such a powder could then prove useful in conferring superhydrophobicity to any surface to which it is applied. To test this concept, the material was then coated onto a glass substrate and adhesive tape and the superhydrophobic properties can be well kept (Figure 11). This observation

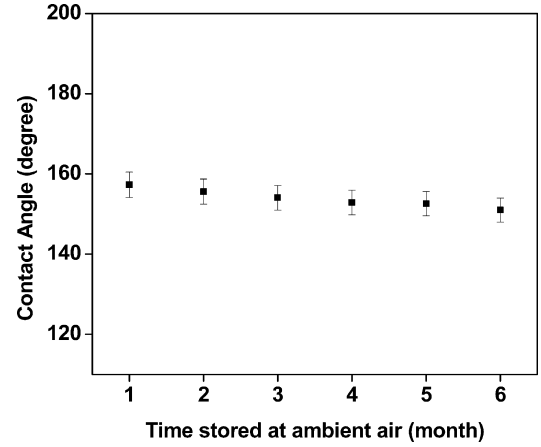

FIGURE 10. Water CA change with time when the CuI-coated silicon wafer was kept in air. Each point represents the mean ± 2% standard error.

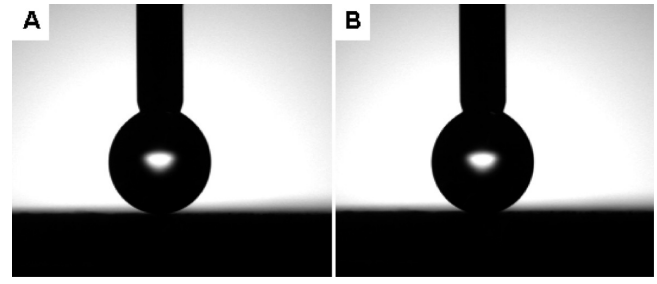

FIGURE 11. CAs of the glass substrate (A) and adhesive tape (B) coated by the as-prepared CuI.

verifies the transferability of the superhydrophobic powder and conceptually opens up a new door in the wettability field.

4. CONCLUSION

In summary, we obtained a superhydrophobic material with a water CA of 157.3° by using a facile wet-chemical process based on CuI, a nonoxide inorganic semiconductor. The surface possesses a hierarchical morphology with two length-scale roughnesses. The excellent water repellency without modification is indicative of the critical role of the two-scale hierarchical morphology, which combines microscale and nanoscale features. More interestingly, the superhydrophobicity of the as-prepared CuI powder is a bulk property of the material and not just of its surface and so could then prove useful in conferring superhydrophobicity to other surfaces to which it is applied. These results provide insight into the design of stable water-repellent surfaces in other powder materials, thus creating opportunities for various exciting applications.

Acknowledgment. This work was supported by the National Natural Science Foundation of China (Grants 50601026 and 20571025), the Henan Provincial Natural Science Foundation of China (Grants 082300420180 and 092300410196), the Natural Science Foundation of Educational Department of Henan Province (Grant 2008A150014), and the Anhui Provincial Natural Science Foundation of China (Grant 070414199).

REFERENCES AND NOTES

(1) Quere, D. *Rep. Prog. Phys.* **2005**, *68*, 2495.
(2) Callies, M.; Quere, D. *Soft Matter* **2005**, *1*, 55.
(3) Genzer, J.; Efimenko, K. *Biofouling* **2006**, *22*, 339.
(4) Jiang, L.; Wang, R.; Yang, B.; Li, T. J.; Tryk, D. A.; Fujishima, A.; Hashimoto, K.; Zhu, D. B. *Pure Appl. Chem.* **2000**, *72*, 73.
(5) Aussillous, P.; QuLrL, D. *Nature* **2001**, *411*, 924.
(6) Wenzel, R. N. *Ind. Eng. Chem.* **1936**, *28*, 988.
(7) Hozumi, A.; Takai, O. *Thin Solid Films* **1997**, *303*, 222.
(8) Cassie, A. B. D. *Discuss. Faraday Soc.* **1948**, *3*, 11.
(9) Wolansky, G.; Marmur, A. *Langmuir* **1998**, *14*, 5292.
(10) Swain, P. S.; Lipowsky, R. *Langmuir* **1998**, *14*, 6772.
(11) Herminghaus, S. *Europhys. Lett.* **2000**, *52*, 165.
(12) Li, S. H.; Li, H. J.; Wang, X. B.; Song, Y. L.; Liu, Y. Q.; Jiang, L.; Zhu, D. B. *J. Phys. Chem. B* **2002**, *106*, 9274.
(13) Genzer, J.; Efimenko, K. *Science* **2000**, *290*, 2130.
(14) Erbil, H. Y.; Demirel, A. L.; Avci, Y.; Mert, O. *Science* **2003**, *299*, 1377.
(15) Mner, D.; McCarthy, T. J. *Langmuir* **2000**, *16*, 7777.
(16) Tsujii, T.; Yamamoto, T.; Onda, T.; Shibuichi, S. *Angew. Chem., Int. Ed. Engl.* **1997**, *36*, 1011.
(17) Tadanaga, K.; Katata, N.; Minami, T. *J. Am. Ceram. Soc.* **1997**, *80*, 3213.
(18) Bico, J.; Marzolin, C.; QuLrL, D. *Europhys. Lett.* **1999**, *47*, 220.
(19) Feng, L.; Yang, Z.; Zhai, J.; Song, Y.; Liu, B.; Ma, Y.; Yang, Z.; Jiang, L.; Zhu, D. *Angew. Chem., Int. Ed.* **2003**, *42*, 4217.
(20) Song, W.; Veiga, D. D.; Custódio, C. A.; Mano, J. F. *Adv. Mater.* **2009**, *21*, published online.
(21) Li, X. M.; Reinhoudt, D.; Crego-Calama, M. *Chem. Soc. Rev.* **2007**, *36*, 1350.
(22) Shirtcliffe, N. J.; McHale, G.; Newton, M. I.; Chabrol, G.; Perry, C. C. *Adv. Mater.* **2004**, *16*, 1929.
(23) Nosonovsky, M.; Bhushan, B. *Adv. Funct. Mater.* **2008**, *18* 843.
(24) Sun, T. L.; Feng, L.; Gao, X. F.; Jiang, L. *Acc. Chem. Res.* **2005**, *38*, 644.
(25) Koch, K.; Bhushan, B.; Barthlott, W. *Soft Matter* **2008**, *4* 1943.
(26) Zhang, X.; Shi, F.; Niu, J.; Jiang, Y.; Wang, Z. *J. Mater. Chem.* **2008**, *18*, 621.
(27) Tuteja, A.; Choi, W.; McKinley, G. H.; Cohen, R. E.; Rubner, M. F. *Mater. Res. Bull.* **2008**, *33*, 752.
(28) Dorrer, C.; Ruhe, J. *Adv. Mater.* **2008**, *20*, 159.
(29) Pastine, S.; Okawa, D.; Kessler, B.; Rolandi, M.; Llorente, M.; Zettl, A.; Fréchet, J. M. J. *J. Am. Chem. Soc.* **2008**, *130*, 4238.
(30) Ma, M. L.; Hill, R. M. *Curr. Opin. Colloid Interface Sci.* **2006**, *11*, 193.
(31) Zhang, X.; Zhao, N.; Liang, S.; Lu, X.; Zhang, X.; Xu, J. *Adv. Mater.* **2008**, *20*, 2938.
(32) Levkin, P. A.; Svec, F.; Fréchet, J. M. J. *Adv. Funct. Mater.* **2009**, *19*, published online.
(33) Onda, T.; Shibuichi, S.; Satoh, N.; Tsujii, K. *Langmuir* **1996**, *12*, 2125.
(34) Shibuichi, S.; Onda, T.; Satoh, N.; Tsujii, K. *J. Phys. Chem.* **1996**, *100*, 19512.
(35) Wu, Y.; Sugimura, H.; Inoue, Y.; Takai, O. *Chem. Vap. Deposition* **2002**, *8*, 47.
(36) Shibuichi, S.; Yamamoto, T.; Onda, T.; Tsujii, K. *J. Colloid Interface Sci.* **1998**, *208*, 287.
(37) Nakajima, A.; Fujishima, A.; Hashimoto, K.; Watanabe, T. *Adv. Mater.* **1999**, *11*, 1365.
(38) Nakajima, A.; Abe, K.; Hashimoto, K.; Watanable, T. *Thin Solid Films* **2000**, *376*, 140.
(39) Tadanaga, K.; Katata, N.; Minami, T. *J. Am. Ceram. Soc.* **1997**, *80*, 1040.
(40) Tada, H.; Nagayama, H. *Langmuir* **1995**, *11*, 136.
(41) Gu, Z. Z.; Uetsuka, H.; Takahashi, K.; Nakajima, R.; Onishi, H.; Fujishima, A.; Sato, O. *Angew. Chem., Int. Ed.* **2003**, *42*, 894.
(42) Huang, X. J.; O'Mahony, A. M.; Compton, R. G. *Small* **2009**, *5*, 776.
(43) Li, H. J.; Wang, X. B.; Song, Y. L.; Liu, Y. Q.; Li, Q. S.; Jiang, L.; Zhu, D. B. *Angew. Chem., Int. Ed.* **2001**, *40*, 1743.
(44) Feng, L.; Li, S. H.; Li, H. J.; Zhai, J.; Song, Y. L.; Jiang, L.; Zhu, D. B. *Angew. Chem., Int. Ed.* **2002**, *41*, 1221.
(45) Feng, L.; Song, Y. L.; Zhai, J.; Xu, J.; Jiang, L.; Zhu, D. B. *Angew. Chem., Int. Ed.* **2003**, *42*, 800.
(46) Feraoun, H.; Aourag, H.; Certier, M. *Mater. Chem. Phys.* **2003**, *82*, 597.
(47) Bouhafs, B.; Heireche, H.; Sekkal, W.; Aourag, H.; Certier, M. *Phys. Lett. A* **1998**, *240*, 257.
(48) Sekkal, W.; Zaoui, A. *Phys. B (Amsterdam, Neth.)* **2002**, *315*, 201.
(49) Liu, Y.; Zhan, J.; Zeng, J.; Qian, Y.; Tang, K.; Yu, W. *J. Mater. Sci. Lett.* **2001**, *20*, 1865.
(50) Perera, V. P. S.; Tennakone, K. *Sol. Energy Mater. Sol. Cells* **2003**, *79*, 249.
(51) Yang, M.; Xu, J.-Z.; Xu, S.; Zhu, J.-J.; Chen, H.-Y. *Inorg. Chem. Commun.* **2004**, *7*, 628.
(52) Takeda, T.; Matsuaga, K.; Uruga, T.; Takakura, M.; Fujiwara, T. *Tetrahedron Lett.* **1997**, *38*, 2879.
(53) Tanji, A.; Akai, I.; Kojima, K.; Karasawa, T.; Komatsu, T. *J. Lumin.* **2000**, *87*, 516.
(54) Tennakone, K.; Kumara, G. R.; Kottedoda, I. R.; Perera, V. P.; Aponsu, G. M.; Wijayantha, K. G. *Sol. Energy Mater. Sol. Cells* **1998**, *55*, 283.
(55) Li, W. J.; Shi, E. W. *Cryst. Res. Technol.* **2002**, *37*, 1041.
(56) Zhang, L. P.; Guo, F.; Liu, X. Z. *Mater. Res. Bull.* **2006**, *41*, 905.
(57) Zhou, Y.; Lü, M.; Zhou, G.; Wang, S.; Wang, S. *Mater. Lett.* **2006**, *60*, 2184.
(58) Ng, C. H. B.; Fan, W. Y. *J. Phys. Chem. C* **2007**, *111*, 9166.
(59) Li, X.; Wang, X. M. *Cryst. Growth. Des.* **2006**, *6*, 2661.
(60) Klapars, A.; Buchwald, S. L. *J. Am. Chem. Soc.* **2002**, *124*, 14844.
(61) Kwong, F. Y.; Klapars, A.; Buchwald, S. L. *Org. Lett.* **2002**, *4*, 581.
(62) Zhu, W.; Ma, D. *Org. Lett.* **2006**, *8*, 261.
(63) Kirsch, P. D.; Ekerdt, J. G. *J. Appl. Phys.* **2001**, *90*, 4256.
(64) Jin, R. C.; Cao, Y. C.; Hao, E.; Métraux, G. S.; Schatz, G. C.; Mirkin, C. A. *Nature* **2003**, *425*, 487.
(65) Li, C.; Cai, W.; Cao, B.; Sun, F.; Li, Y.; Kan, C.; Zhang, L. *Adv. Funct. Mater.* **2006**, *16*, 83.
(66) Li, Y.; Huang, X. J.; Heo, S. H.; Li, C. C.; Choi, Y. K.; Cai, W. P.; Cho, S. O. *Langmuir* **2007**, *23*, 2169.
(67) Ren, H.-X.; Huang, X.-J.; Yarimaga, O.; Choi, Y.-K.; Gu, N. *J. Colloid Interface Sci.* **2009**, *334*, 103.
(68) Li, Y.; Cai, W.; Duan, G.; Cao, B.; Sun, F.; Lu, F. *J. Colloid Interface Sci.* **2005**, *287*, 634.

AM900466F